Clin Physiol Funct Imaging (2017) 37, pp52–61 doi: 10.1111/cpf.12267

# An echo-planar imaging sequence is superior to a steady-state free precession sequence for visual as well as quantitative assessment of cardiac magnetic resonance stress perfusion

Britt-Marie Ahlander[1], Eva Maret[1,2], Lars Brudin[3], Sven-Ake Starck[4,5] and Jan Engvall[6,7,8]

[1]Department of Radiology, Ryhov County Hospital, Jonkoping, [2]Department of Clinical Physiology, Karolinska University Hospital, Stockholm, [3]Department of Clinical Physiology, Kalmar County Hospital, Kalmar, [4]Department of Natural Science and Biomedicine, School of Health Sciences, Jonkoping University, [5]Department of Oncology, Hospital Physics, Ryhov County Hospital, Jonkoping, [6]Department of Medical and Health Sciences, Linkoping University, [7]Department of Clinical Physiology, County Council of Ostergotland, and [8]Center of Medical Image Science and Visualisation, Linkoping University, Linkoping Sweden

**Correspondence**
Jan Engvall, Center of Medical Image Science and Visualisation, Linkoping University, SE-581 83 Linkoping, Sweden.
E-mail: jan.engvall@regionostergotland.se

**Accepted for publication**
Received 7 November 2014;
accepted 8 May 2015

**Key words**
cardiac imaging techniques; coronary heart disease; Magnetic Resonance Imaging; nuclear medicine; perfusion

## Summary

*Background* To assess myocardial perfusion, steady-state free precession cardiac magnetic resonance (SSFP, CMR) was compared with gradient-echo–echo-planar imaging (GRE-EPI) using myocardial perfusion scintigraphy (MPS) as reference.
*Methods* Cardiac magnetic resonance perfusion was recorded in 30 patients with SSFP and in another 30 patients with GRE-EPI. Timing and extent of inflow delay to the myocardium was visually assessed. Signal-to-noise (SNR) and contrast-to-noise (CNR) ratios were calculated. Myocardial scar was visualized with a phase-sensitive inversion recovery sequence (PSIR). All scar positive segments were considered pathologic. In MPS, stress and rest images were used as in clinical reporting. The CMR contrast wash-in slope was calculated and compared with the stress score from the MPS examination. CMR scar, CMR perfusion and MPS were assessed separately by one expert for each method who was blinded to other aspects of the study.
*Results* Visual assessment of CMR had a sensitivity for the detection of an abnormal MPS at 78% (SSFP) versus 91% (GRE-EPI) and a specificity of 58% (SSFP) versus 84% (GRE-EPI). Kappa statistics for SSFP and MPS was 0·29, for GRE-EPI and MPS 0·72. The ANOVA of CMR perfusion slopes for all segments versus MPS score (four levels based on MPS) had correlation r = 0·64 (SSFP) and r = 0·96 (GRE-EPI). SNR was for normal segments 35·63 ± 11·80 (SSFP) and 17·98 ± 8·31 (GRE-EPI), while CNR was 28·79 ± 10·43 (SSFP) and 13·06 ± 7·61 (GRE-EPI).
*Conclusion* GRE-EPI displayed higher agreement with the MPS results than SSFP despite significantly lower signal intensity, SNR and CNR.

## Introduction

Myocardial ischaemia can be detected by the difference in myocardial signal intensity on cardiac magnetic resonance images recorded after stress and at rest. Normally, the extraction of oxygen in the myocardium is high, and an increase in myocardial oxygen demand requires an increase in coronary blood flow. In coronary arteries with a normal endothelial function and normal cross-sectional area, coronary blood flow may increase four times the resting level during vasodilation or dynamic exercise. This increase in flow is reported as coronary flow reserve (CFR) (Gould *et al.*, 1990). The coronary vasculature in the perfusion area supplied by a stenotic vessel is already maximally dilated and displays a reduced response to the injection of adenosine in comparison with other myocardial segments. This mechanism is utilized for imaging differences between stress and rest perfusion with CMR, and with MPS using single photon emission computed tomography (SPECT) (Fleischmann *et al.*, 2004; Gibbons *et al.*, 2006), Fig. 1.

Myocardial perfusion scintigraphy is the pre-eminent clinical method for the evaluation of myocardial perfusion and

  

uses exercise-induced flow reduction or the redistribution of flow from pharmacological vasodilation to define pathologic segments from those considered normal. The method has a reasonable diagnostic accuracy but requires the administration of radionuclide tracers (Zhang *et al.*, 1998; Fleischmann *et al.*, 2004; Gibbons *et al.*, 2006; Marcassa *et al.*, 2008) that will cause some radiation exposure to the patient.

Cardiac magnetic resonance imaging has emerged as an important method for the evaluation of coronary artery disease (CAD). It has a high spatial resolution, good signal-to-noise (SNR) and contrast-to-noise ratios (CNR) and requires neither X-rays nor radiotracers (Constantine *et al.*, 2004; Nandalur *et al.*, 2007; Greenwood *et al.*, 2011). Late gadolinium enhancement (LGE) imaging is the gold standard (Sakuma, 2007) for visualizing myocardial scar. After intravenous injection, gadolinium accumulates in the extracellular space in fibrotic non-viable myocardium and washes out slowly, enhancing the magnetic resonance (MR) signal of scar tissue by shortening the T1 relaxation time (Finn *et al.*, 2006; Sakuma, 2007). In first pass perfusion imaging, a contrast bolus traverses the pulmonary circulation and the left ventricle to produce an increase in MR signal in the left ventricular wall. Gadolinium contrast material in highly perfused myocardium appears bright, while hypoperfused areas have less (darker) signal (Barkhausen *et al.*, 2004; Gerber *et al.*, 2008; Kim *et al.*, 2009). This difference in signal intensity (SI) can be evaluated visually, semiquantitatively or quantitatively (Gerber *et al.*, 2008; Jerosch-Herold, 2010), Fig. 2. Visual assessment is fast but requires experienced investigators that can differentiate true perfusion reduction from 'dark rim' artefact (Di Bella *et al.*, 2005), Fig. 3. Objective measurements to detect segmental ischaemia are based on, for example, stress–rest differences in the slope of the signal intensity curve of the myocardium or a reduction in subendocardial compared to epicardial blood flow using Fermi deconvolution to determine absolute blood flow (Mordini *et al.*, 2014).

Magnetic resonance sequences used for perfusion need to have a high temporal and spatial resolution. Three short axis slices with six segments in each slice (Cerqueira *et al.*, 2002) cover all three levels of the left ventricle (excluding the apical cap). Strong T1 weighting is required for visualization of differences in contrast density (Kellman and Arai, 2007). Perfusion sequences have been designed based on gradient-echo–echo-planar imaging, GRE-EPI, or steady-state free precession, SSFP (Kellman and Arai, 2007; Gerber *et al.*, 2008). Based on the properties of SSFP, with a high SNR and CNR, we hypothesized that an SSFP sequence could have advantages in cardiac perfusion compared with the GRE-EPI sequence (Wang *et al.*, 2005; Gebker *et al.*, 2007; Merkle *et al.*, 2007).

The aim of this study was to compare first pass stress myocardial perfusion CMR, obtained with two different sequences, with each other using the result from the MPS stress study as reference. Angiography was not part of the study and was later available only for seven of the 60 patients.

## Methods

### Patients

Sixty patients (mean age 62 years, range 37–80, 23 women), Table 1, referred for MPS for myocardial ischaemia were

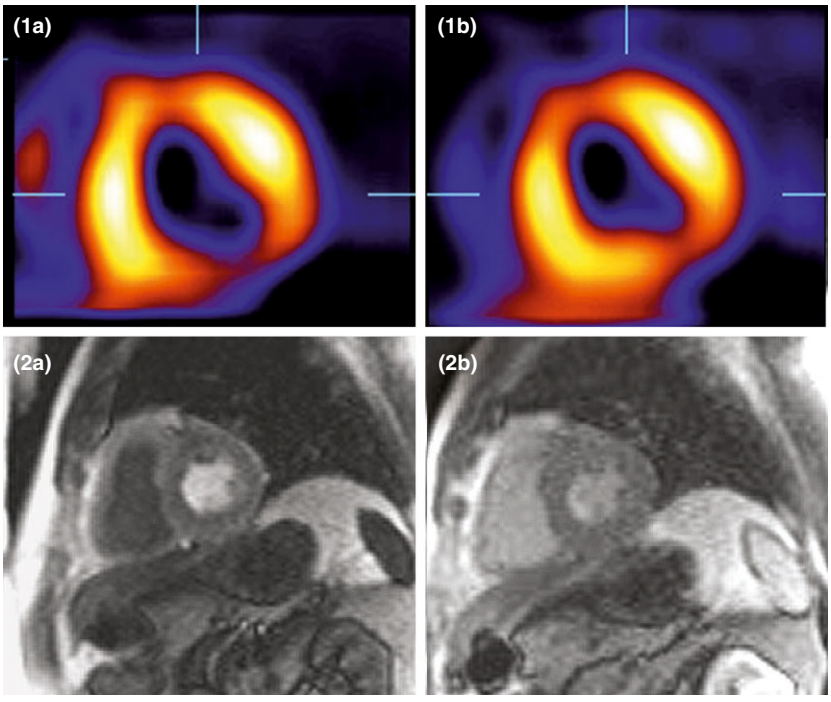


**Figure 1** SPECT (1a and 1b) and CMR GRE-EPI (2a and 2b) images of reversible myocardial ischaemia. Stress is 'a' and rest 'b'.

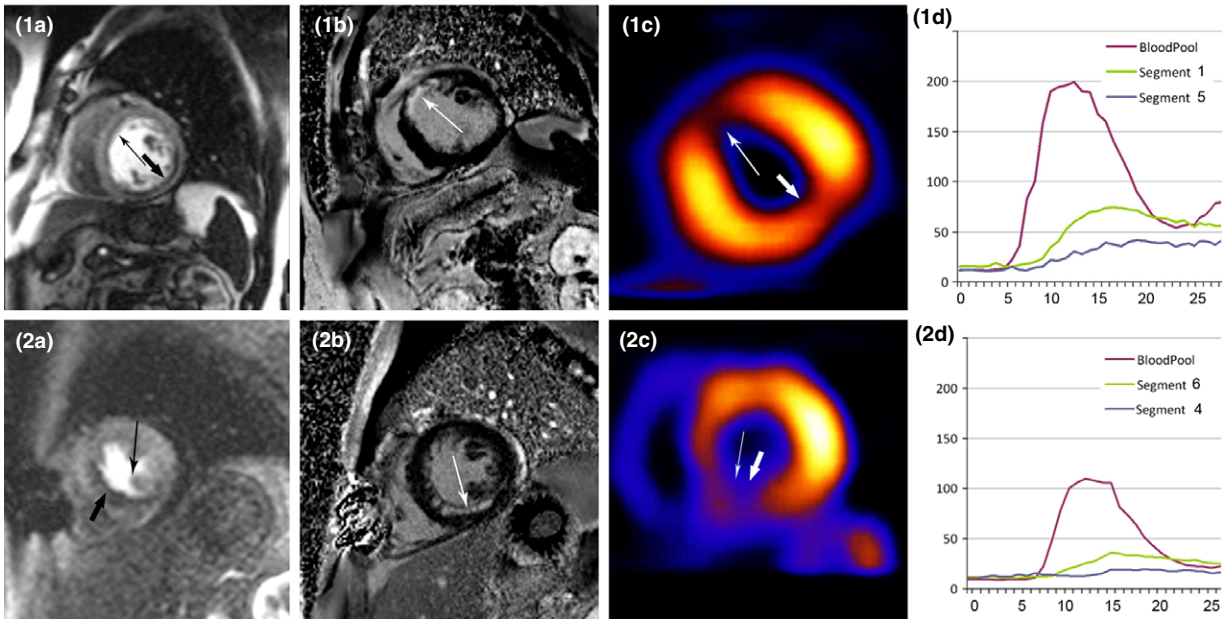


**Figure 2** Composite image of two patient studies with ischaemia and myocardial scar, SSFP in 1 and GRE-EPI in 2. Perfusion with SSFP sequence (1a), anteroseptal scar visualized with LGE sequence (1b), corresponding MPS image (1c) and contrast wash-in curves (1d) for the bloodpool (red), a pathologic segment (blue) and a normal segment (green). Perfusion with GRE-EPI sequence (2a), inferoseptal scar (2b), MPS image (2c) and wash-in curves (2d). Annotation as in 1d. Segment numbers according to SCMR. Scar is indicated by thin arrows and ischaemia by thick arrows. In wash-in curves, MRI contrast signal intensity is depicted on the *y*-axis and time (s) on the *x*-axis.

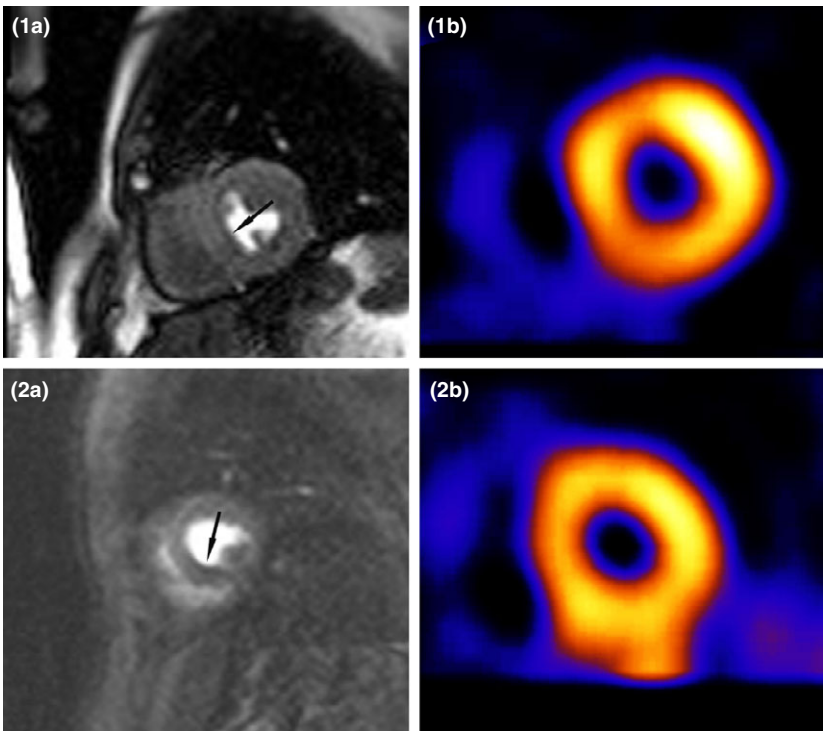


**Figure 3** Dark rim artefact at arrows on CMR perfusion images using SSFP (1a) and GRE-EPI (2a) sequences. Corresponding normal MPS images (1b and 2b). Slight extracardiac bowel isotope uptake signal in 2b.

enrolled in the study between April 2008 and June 2011. In the initial phase from April 2008 to April 2009 30, patients were investigated with an SSFP sequence, while in the period between November 2009 and June 2011 30, patients were investigated with the GRE-EPI sequence. Exclusion criteria were as follows: contraindications for magnetic resonance imaging, to the use of adenosine vasodilator or gadolinium contrast, inability to communicate or unwillingness to participate.

The study was approved by the regional ethical review board in Linköping, Sweden, and adhered to Good Clinical

**Table 1** Clinical characteristics for the 30 patients in each MR perfusion group; steady-state free precession (SSFP) and gradient-echo–echo-planar imaging (GRE-EPI).

| Characteristics | SSFP ($n$ = 30) | GRE-EPI ($n$ = 30) | $P$-value[a] |
|---|---|---|---|
| Gender n (%) | | | |
| Male | 17 (57) | 20 (67) | |
| Female | 13 (43) | 10 (33) | 0·595 |
| Age year; mean (SD) | 60 (9·3) | 64 (10·3) | 0·051 |
| BMI kg $m^{-2}$; mean (SD) | 26 (4·2) | 27 (3·6) | 0·273 |
| Diabetes n (%) | 3 (10) | 7 (23) | 0·490 |
| Hypertension n (%) | 14 (47) | 21 (70) | 0·115 |
| Smoker n (%) | 5 (17) | 4 (13) | 0·735 |
| Ischaemic heart disease n (%) | 26 (87) | 29 (97) | 0·353 |
| Angina pectoris | 25 (83) | 29 (97) | 0·194 |
| Infarction | 8 (27) | 15 (50) | 0·110 |
| PCI | 9 (30) | 10 (33) | >0·9 |
| CBAG | 4 (13) | 3 (10) | >0·9 |
| Peripheral vascular disease n (%) | 7 (23) | 2 (7) | 0·145 |
| Medication n (%) | | | |
| Betablocker | 17 (57) | 21 (70) | 0·422 |
| Calcium | 7 (23) | 11 (37) | 0·398 |
| Statin | 19 (63) | 17 (57) | 0·792 |
| ACI-I | 10 (33) | 18 (60) | 0·069 |
| Blood pressure; mean (SD) | | | |
| Systolic | 137 (21·9) | 140 (19·2) | 0·730 |
| Diastolic | 78 (12·1) | 77 (9·6) | 0·476 |
| Follow-up n (%)[b] | | | |
| MI | 4 (13) | 3 (10) | >0·9 |
| PCI | 7 (23) | 4 (13) | 0·506 |
| Angiography | 6 (20) | 3 (10) | 0·471 |
| CABG | 0 (0) | 1 (3) | >0·9 |

[a]Differences between groups analysed using Mann–Whitney non-parametric U-test for continuous parameters and Fisher's exact test for categorical (frequencies).
[b]Follow-up is performed April 2015, 7–4 years after CMR.

Practice as set forth in the declaration of Helsinki. Written informed consent was obtained from all patients after the nature of the procedures had been fully explained.

## Cardiac Magnetic Resonance Imaging

All examinations were performed on an 1·5-T MRI scanner (Magnetom Avanto; Siemens Healthcare, Erlangen, Germany) with a 6-element phased array body matrix coil combined with six elements in the spine coil, altogether 12 elements. All images were acquired in supine position and in end diastole during breathhold. Gadopentetate dimeglumine contrast 0·5 mmol $ml^{-1}$ (Magnevist; Bayer Schering Pharma, Berlin, Germany) and adenosine 5 mg $ml^{-1}$ (Item Development AB, Stocksund, Sweden) was used for stress imaging. Electrocardiogram (ECG) and heart rate were monitored during the entire examination, while blood pressure was checked only before the patient entered the scanner room. After scout images, the scanning table was moved outside the tunnel to facilitate control of side effects and the adenosine infusion was started (140 μg min per kg body weight). Patients had been instructed to withhold caffeine for 24 h (Carlsson *et al.*, 2014). After three minutes, 99m Tc tetrofosmin (for the MPS study) was given followed by a sodium chloride chaser and the table moved to the scanning position. When the correct scanning position was reached, 8 ml gadolinium contrast was infused using a power injector (Medrad Inc, Indianola, PA, USA) at a rate of 4 ml $s^{-1}$ during breathhold, while the vasodilator infusion was still running.

For perfusion analysis, three 8-mm-thick short axis images were equally spaced along the left ventricular long axis in the middle position of the basal, mid- and apical segments. The perfusion sequences were ECG-gated with non-selective saturation recovery preparation pulses. The sequence parameters for SSFP were TR/TE/TI/FA 172·7/1·11/100 ms/50°, raw data matrix 60 × 160, field of view (FOV) 250 × 380 $mm^2$, bandwidth (BW) 1359 Hz per pixel and voxel spatial resolution 3·2 × 2·4 × 8 $mm^3$. Depending on patient size, FOV varied from 225 × 300 to 330 × 440 $mm^2$ and pixel size from 2·5 × 1·9 to 3·7 × 2·8 $mm^2$. For GRE-EPI, the parameters were TR/TE/TI/FA 146·95/1·26/115 ms/20°, raw data matrix of 102 × 128, FOV 281 × 360 $mm^2$, BW1628 Hz/pixel and voxel spatial resolution 3·5 × 2·8 × 8 $mm^3$. In this sequence, FOV varied from 273 × 350 to 351 × 450 $mm^2$ resulting in a pixel size of 2·7 × 3·3–3·5 × 4·4 $mm^2$. Parallel imaging, GeneRalized Autocalibrating Partially Parallel Acquisition (GRAPPA) (Griswold *et al.*, 2002), with an acceleration factor 2, was used in the phase-encoding direction. First pass perfusion images at rest were acquired 10 min after the stress study using a second bolus of 8 ml gadolinium contrast and identical scanner settings. The perfusion contrast dose corresponded to 0·05 mmol $kg^{-1}$ for an 80 kg individual which is a dose recommended by SCMR (Kramer *et al.*, 2008). For scar imaging, a third contrast injection was given aiming at a total contrast dose of 0·2 mmol $kg^{-1}$. However, for practical reasons, a maximal dose of 30 ml was used. 28 of the 60 patients weighed more than 75 kg and were subject to this limitation in dosage. Cine images for ventricular function and LGE images for scar evaluation were acquired before the patient moved to the nuclear department where MPS was performed about 60 min after the injection of the radiotracer.

## Image analysis of first pass perfusion CMR

Image analysis was performed after the conclusion of the study, on the entire batch of study patients. First pass perfusion CMR during stress and at rest was qualitatively evaluated using visual assessment of the presence of delayed wash-in of contrast. Ischaemia was deemed likely if the delay was not being present in the rest images, and artefact was deemed likely if the reduction was short-lived (four beats or less) and affected a shallow depth of the LV wall (Hundley *et al.*, 2009). The level of diagnostic confidence was given on a four-point scale: (i) normal with high confidence, (ii) normal

with low confidence, (iii) pathologic with low confidence and (iv) pathologic with a high confidence (Schwitter *et al.*, 2008). A difference of two steps between stress and rest was required to determine that a specific segment was ischaemic. In the semiquantitative evaluation, the slope of the signal increase in the myocardium was measured on a work station using 'Argus Dynamic Signal™' (Siemens Healthcare). Each slice was automatically divided into six segments, creating 18 (3 × 6) segments in every patient excluding the apical cap. Thus, the evaluation differed slightly from the 17-segment model recommended by the American Heart Association (Taylor *et al.*, 2010). The epicardial and endocardial borders were manually segmented excluding the high signal of blood in the cavity and the epicardial fat surrounding the left ventricle. Segmentation was repeated for each time step and the signal intensity curve recorded for each segment. The slope of the inflow signal was calculated between the foot and the peak of the curve; thus, the derivative of the slope was not used.

Reproducibility for the slope measurement was based on two independent observers evaluating five patients each for both sequences. Qualitative evaluation of first pass perfusion CMR was performed by an experienced reader of cardiac MRI (>10 years) who was blinded to the MPS result. To optimize specificity and sensitivity, LGE images were used to identify areas of scar. An LGE positive segment was always considered pathological (Kramer, 2006).

For each patient, SNR and CNR were calculated in the anterior segment of the basal left ventricle when healthy and in all ischaemic segments, before and after the infusion of gadolinium contrast, for both perfusion sequences. Baseline SI was chosen as the value before the start of the infusion and peak SI as the highest value during contrast infusion. Noise was defined as the standard deviation of the signal in air outside the patient. SNR was calculated by dividing SI with noise. CNR for the contrast enhanced myocardium during perfusion compared with the myocardium before perfusion was calculated as $(SI_{Myocard\ perfusion} - SI_{Myocard\ baseline})$/noise.

## Myocardial perfusion scintigraphy

The perfusion images from the stress study were used for evaluation. During adenosine stress in the MR scanner, 5·7 MBq $^{99m}$Tc tetrofosmin per kg bodyweight was given i.v. (max 570 MBq) (Myoview™, GE-Healthcare Medi-Physics, Inc, Arlington Heights, IL, USA). MPS imaging commenced 60 min after injection of the radiotracer. A dual-detector gamma camera (E. CAM; Siemens Medical Systems Inc, Hoffman Estates, IL, USA) equipped with a high resolution collimator was used. Thirty-two views were acquired in steps of 2·8 degrees per detector, and the acquisition time/angle was 30 s. A 19% window was 'asymmetrically placed' (129–155 keV) on the 140 keV peak. A 64 × 64 word matrix with a pixel size of 6·6 mm was used. The studies were acquired simultaneously in both non-gated and ECG-gated mode.

## Image analysis of myocardial perfusion scintigraphy

The non-gated acquisition files were reconstructed using filtered back projection, prefiltered with a Butterworth filter (cut-off 0·8 $cm^{-1}$, order 10), (Hermes Medical Solutions, Stockholm, Sweden). The images were realigned into short axis slices in two phases, transverse rotation followed by oblique rotation. In case of interfering bowel uptake, acquisition was repeated after intake of fluids. Attenuation correction or prone imaging was not performed.

The images were analysed with QGS-QPS Quantitative Perfusion SPECT (Cedars-Sinai Medical Center, Los Angeles, CA, USA). The stress perfusion polar map was divided in 20 segments, six in each basal, mid- and apical area and two segments in the apex. The apical segments were not used as the CMR method could not visualize this area. Stress scores were given according to reference standards incorporated in the QPS software (based on segmental differences in signal intensity as seen in a healthy reference population). Using these scores, segments were reported as (0) normal, (1) probably normal, (2) probably diseased and (3 and 4) definitely diseased. For the visual comparison, both stress and rest images were used and assessed by an experienced nuclear physician (>10 years of experience) who was blinded to the results of the evaluation of MR perfusion.

## Statistics

Descriptive statistics was used for both qualitative and quantitative evaluation of the agreement between the two CMR sequences in relation to MPS. For visual assessment, on a patient level, cross-tabulation of the binary data (normal-ischaemic/scar CMR and normal reversible/not reversible MPS) was performed. For proportion of agreement between MPS and SSFP and GRE-EPI respectively, kappa was calculated (Landis and Koch 1977). Sensitivity and specificity for detecting patients with ischaemic heart disease, with MPS as reference, was calculated for both sequences. Intraclass correlation with 95% confidence interval was used for the calculation of interobserver variability. According to the Kolmogorov–Smirnov and Shapiro–Wilk tests, the distribution of CMR slope as well as MPS scores was skewed which necessitated values to be normalized to the peak value in each individual giving symmetrical and well-normalized distributions. The contrast wash-in slope was calculated for each segment and compared with the stress score from the MPS examination, using ANOVA. Region (basal, middle and apical), total number of segments, stress score and patient were used as input parameters.

Student's t-test for independent samples was used for comparison between the sequences regarding SI, SNR and CNR. A P-value $\leq 0{\cdot}05$ was considered significant. All analyses were performed using Statistica version 10 (Statsoft Inc. Tulsa, OK, USA).

## Results

### Patients

Sixty seven patients were initially enrolled of which seven were excluded for the following reasons: lack of two venous access lines (1), claustrophobia (4), scanner problem (1), arrhythmia (1). Patient mean age was 62 ± 10 years, and 23 were women. Patients in the group examined with GRE-EPI were slightly older, had a higher proportion of diabetes, hypertension and previous infarction, Table 1. Peripheral vascular disease was more frequent in the group examined with the SSFP sequence.

### Effects of adenosine

The administration of adenosine increased heart rate from 64 ± 12 to 89 ± 14 (SSFP) and from 63 ± 10 to 83 ± 16 (GRE-EPI). All patients had an increase in heart rate exceeding 10 beats $min^{-1}$. An increase in heart rate of 10% is frequently seen as the lower limit for an adequate hemodynamic response to vasodilation.

### Late gadolinium enhancement

Myocardial scar was present in 10 pts from each perfusion sequence. For SSFP, the mean scar size/left ventricular mass (LVM) was 7·40% ± 9·03 and for GRE-EPI 7·10% ± 5·51. Scar size did not differ between the two sequences, P = 0·92 (Mann–Whitney U-test).

### Myocardial volumes derived from CMR and MPS

The end-diastolic volume of the left ventricle (LVEDV) derived from CMR was 145 ± 34 ml (SSFP) and 161 ± 43 ml (GRE-EPI). Left ventricle ejection fraction (EF) was 58 ± 11% (SSFP) and 61 ± 11% (GRE-EPI). Using MPS, LVEDV was 107 ± 43 ml (SSFP) and 115 ± 51 ml (GRE-EPI). Ejection fraction was 54 ± 11% (SSFP) and 56 ± 11% (GRE-EPI), Table 2. Ejection fraction and volume measurements were not statistically different between the two MR cohorts (P>0·05).

**Table 2** End-diastolic volume and ejection fraction measured with CMR and MPS for the two sequence groups. Measurements are mean value ± SD.

| | SSFP[a] | GRE-EPI[b] | *P*-value |
|---|---|---|---|
| SPECT LVEDV ml | 107 ± 43 | 115 ± 51 | 0·49 |
| SPECT EF % | 54 ± 11 | 56 ± 11 | 0·37 |
| CMR LVEDV ml | 145 ± 34 | 161 ± 43 | 0·11 |
| CMR EF% | 58 ± 11 | 61 ± 11 | 0·21 |

[a]Steady-state free precession.
[b]Gradient-echo–echo-planar imaging.

### SNR and CNR for the two CMR sequences

At peak gadolinium, signal intensity for normal segments was 67·72 ± 6·40 for SSFP versus 39·43 ± 16·86 for GRE-EPI. SNR and CNR were as expected higher for SSFP than for the GRE-EPI sequence. SNR was for normal segments 35·63 ± 11·80 (SSFP) and 17·98 ± 8·31 (GRE-EPI), while CNR was 28·79 ± 10·43 (SSFP) and 13·06 ± 7·61 (GRE-EPI). But, segments with definite ischaemia (rated 3 or 4) had SNR 32·31 ± 13·31 (SSFP) versus SNR 15·71 ± 7·87 (GRE-EPI), while CNR was 25·18 ± 12·48 (SSFP) and 10·41 ± 7·66 (GRE-EPI). In a comparison of SNR and CNR between the two sequence groups, these pairwise differences were all statistically significant, but the difference in SNR and CNR between normal and ischaemic segments was non-significant for SSFP as well as for GRE-EPI, Table 3.

### Visual assessment of MPS and CMR

Visual assessment of MPS showed signs of coronary artery disease in 20 pats (ischaemia or scar) of which 13 demonstrated reversible ischaemia. The corresponding numbers for the two MRI sequences altogether were 26 and 21, Table 4. Using MPS as reference, the sensitivity for the detection of an abnormal CMR was 78% (SSFP) versus 91% (GRE-EPI), while specificity was 58% (SSFP) and 84% (GRE-EPI). Kappa statistics for the agreement between GRE-EPI and MPS was 0·72 and for SSFP 0·29 (Landis and Koch, 1977), but this was not statistically significant, P = 0·07, Fischer's exact test.

### Quantitative segmental CMR and MPS

The slope of myocardial CMR contrast wash-in during vasodilation was compared with MPS summed stress scores, Fig. 4. For all three levels of the left ventricle, basal, mid- and apex segments with a high MPS stress score had a lower rise in the CMR slope than segments with low MPS stress score. The

**Table 3** SI, SNR and CNR calculated for normal and ischaemic segments, measured in regions where both ischaemic and normal segments were found. CE = contrast enhancement. Measurements are mean value ± SD. Whereas all comparisons between sequences were statistically significant, the difference between normal and ischaemic segments in SNR and CNR was not statistically significant for neither SSFP nor GRE-EPI. Measurements are mean value ± SD.

| | SSFP[a] | GRE-EPI[b] | *P*-value |
|---|---|---|---|
| SI normal CE | 67·72 ± 6·40 | 39·43 ± 16·86 | 0·007 |
| SI ischaemic CE | 62·10 ± 18·35 | 34·72 ± 16·81 | 0·030 |
| SNR normal | 35·63 ± 11·80 | 17·98 ± 8·31 | 0·017 |
| SNR ischaemic | 32·31 ± 13·31 | 15·71 ± 7·87 | 0·030 |
| CNR normal | 28·79 ± 10·43 | 13·06 ± 7,61 | 0·018 |
| CNR ischaemic | 25·18 ± 12·48 | 10·41 ± 7·66 | 0·039 |

[a]Steady-state free precession.
[b]Gradient-echo–echo-planar imaging.

**Table 4** Cross-tabulation of the visual assessment of CMR and MPS. MPS: normal or reversible/irreversible reduction of perfusion. CMR: normal, ischaemia or scar.

| | MPS[b] | | |
|---|---|---|---|
| CMR[a] | Normal | Reversible/ irreversible | Kappa[c] |
| SSFP (%) | | | |
| Normal | 12 (57) | 9 (43) | 0·286 |
| Ischaemic/scar | 2 (22) | 7 (78) | |
| GRE-EPI (%) | | | |
| Normal | 16 (84) | 3 (16) | 0·724 |
| Ischaemic/scar | 1 (9) | 10 (91) | |
| Total (%) | | | |
| Normal | 28 (70) | 12 (30) | 0·494 |
| Ischaemic/scar | 3 (15) | 17 (85) | |

[a]Cardiac magnetic resonance imaging.
[b]Myocardial perfusion scintigraphy.
[c]0–0·2: Poor agreement, >0·2–0·4, fair, >0·4–0·6 moderate, >0·6–0·8 substantial and >0·8 almost perfect agreement. P = 0·07, Fisher's exact test, two sided.

ANOVA of CMR perfusion slopes for all segments of the left ventricle versus MPS score (four points based on MPS classification of segments) had correlation r = 0·64 (SSFP) and r = 0·96 (GRE-EPI).

### Reproducibility

Intraclass correlation between two observers measuring myocardial wash-in slope showed fair agreement of consistency for the GRE-EPI sequence, 0·86 with CI 95% 0·80–0·90. The SSFP sequence showed lower agreement, 0·53 CI 95% 0·36–0·66.

## Discussion

Previous studies have demonstrated that CMR perfusion imaging may be superior to MPS in the detection of myocardial ischaemia and significant coronary stenoses (Merkle *et al.*, 2007; Schwitter *et al.*, 2008, 2012) although CMR yet lacks the clinical prognostic documentation that is available for MPS. Still, there is no consensus regarding which sequence to prefer in CMR perfusion. SSFP was known to have higher SNR and CNR than spoiled gradient and echo-planar imaging (Wang *et al.*, 2005; Gebker *et al.*, 2007; Merkle *et al.*, 2007) which gave hope for an advantage also in perfusion imaging. However, despite similarly high values of SNR and CNR also in this study, the sensitivity and specificity to detect abnormal myocardial perfusion was lower for SSFP compared with GRE-EPI. This was true for quantitative as well as clinical visual assessment. The effect of a T1-shortening agent such as gadolinium on different MR sequences is complex. Flip angle, echo time, repetition time and saturation recovery all interact in a complex manner, but it is likely that a GRE-EPI with a flip angle of 20° confers a stronger T1 weighting than SSFP with a flip angle 50°, depending on the balance between T1 and T2 weighting in SSFP. Some of the superior SNR of SSFP may thus be produced by the combined T1/T2 weighting of balanced SSFP. Likewise, the high concentration of gadolinium contrast enhancement during first pass perfusion shortens both the T1 and the T2* relaxation, which perhaps is a disadvantage in a T1/T2-weighted sequence, where the increase in signal due to T1 can be reduced by the decrease in signal due to T2*.Furthermore, the appearance of artefacts may differ between sequences. SSFP is sensitive to 'dark rim artefact', DRA, which can be mistaken for a perfusion defect. It has been suggested that this artefact may be caused by Gibb's ringing (low resolution in the phase-encoding direction), by cardiac motion, magnetic susceptibility, or T2* effects due to the high concentration of cavity contrast during bolus injection (Di Bella *et al.*, 2005; Gerber *et al.*, 2008). However, there is no consensus as to when the DRA is due to artefact or a true reduction in perfusion (Di Bella *et al.*, 2005). It has been suggested that a short-lived endocardial darkening favours artefact (Barkhausen *et al.*, 2004). Other authors (Hautvast *et al.*, 2011) have tried to circumvent this problem by investigating the perfusion gradient from many (60) sectors along the circumference of the left ventricle. Their method relies on a comparison between stress and rest that effectively nullifies the effect of the DRA, and on the fact that slow wash-in for the entire myocardial thickness increases the likelihood of the presence of a significant stenosis of the supply vessel. Still, significant difficulties remain for determining quantitative measures of CMR perfusion and the assessment of signal from scar areas (Gupta *et al.*, 2012; Bratis and Nagel, 2013). Recently, Arai *et al.* showed that the highest area under curve for the detection of >70% coronary stenosis on quantitative coronary angiography was obtained with a double bolus perfusion technique and absolute quantification of myocardial blood flow, compared with three different semiquantitative techniques, regardless of the presence of scar or not (Mordini *et al.*, 2014). This technique needs to be evaluated in larger studies.

In studies where visual assessment is used, a higher perfusion contrast dose, 0·075–0·1 mmol $kg^{-1}$, has been found to confer increased sensitivity and specificity of CMR perfusion detection of coronary stenoses defined with X-ray coronary angiography (Schwitter *et al.*, 2008). This suggests that contrast dosing should be considered in light of the method of image assessment. While the human eye may be more sensitive to the difference in signal intensity caused by a high contrast dosing, available semiquantitative evaluation methods may not. In our hands, visual assessment was not inferior to quantitative measurements.

The field strength of the scanner is important for the selection of the sequence used for cardiac perfusion imaging, as at 3T, a T1-weighted EPI sequence has twice as high SNR as at 1·5 T (Gutberlet *et al.*, 2006) and the SSFP sequence displays more susceptibility artefacts at 3T compared with 1·5 T

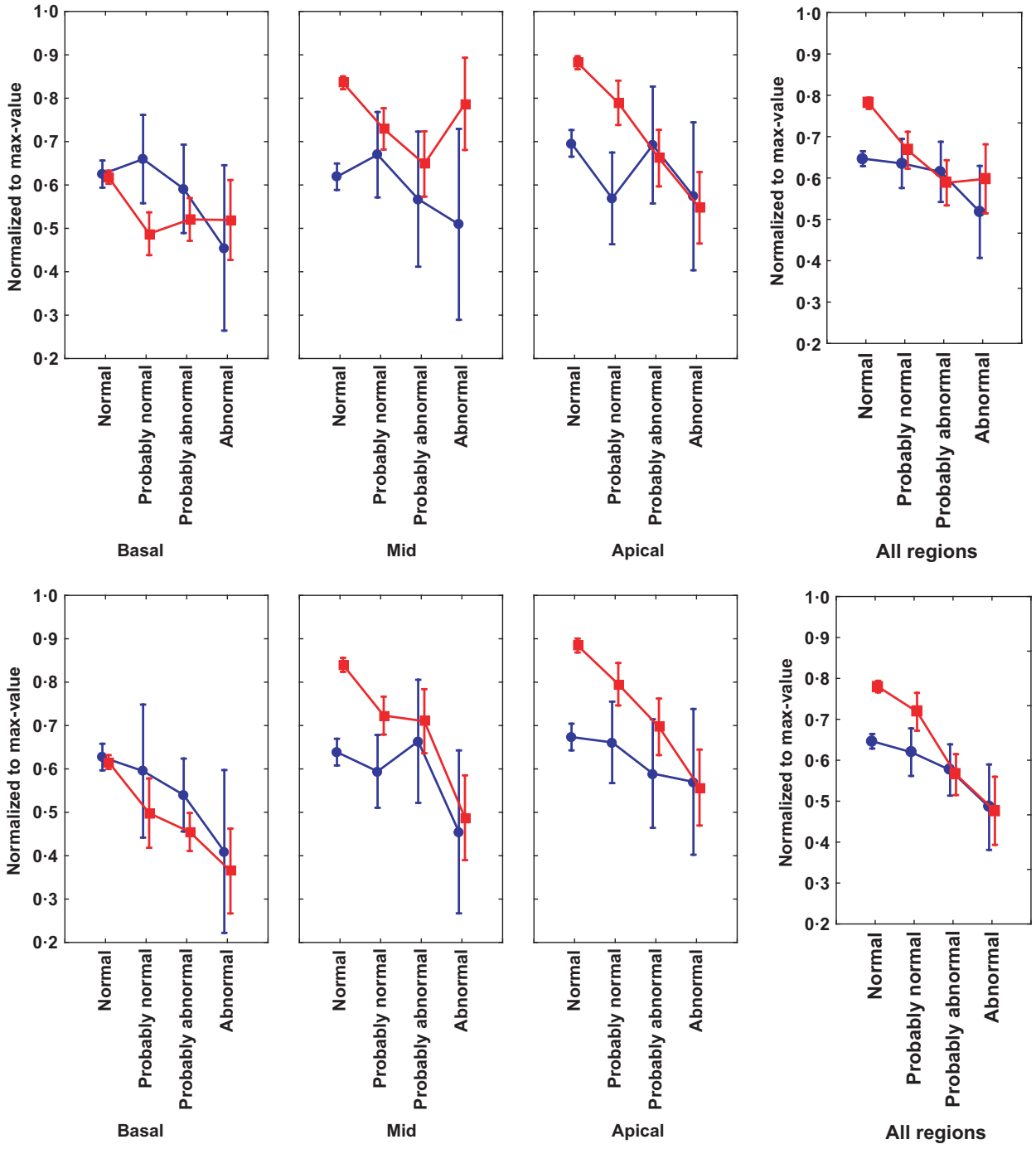


**Figure 4** MPS scores (red line with squares) and MR slope (blue line with dots) during vasodilation. SSFP (upper panels) and GRE-EPI (lower panels). The three segmental levels base, middle and apex to the left and the aggregated results to the right. Values are normalized to maximum value in each individual to allow for comparisons. Normal, ischaemic and scar segments are all included.

(Gerber *et al.*, 2008). This suggests that GRE-EPI might perform even better at 3T.

A number of limitations apply to this study as follows: the two CMR sequences were applied to two different cohorts, as the GRE-EPI sequence became available somewhat later. Even if both sequences had been available simultaneously, the appropriateness of performing two different stress tests on each patient would have been questionable. A head-to-head comparison of the two sequences was therefore not possible. MPS was selected for reference as it exploits the physiologic effect of a coronary stenosis which is the mechanism studied also in MR perfusion, but the sensitivity and specificity of MPS to detect coronary artery stenoses is imperfect even if it has recently been used to validate a 3D MRI perfusion

sequence (Jogiya *et al.*, 2014). Furthermore, as MPS has a dose–response (tracer signal versus flow) relationship that is partly determined by membrane function as well as coronary blood flow, this relationship has nonlinear components which can have added to some of the observed differences between the two perfusion sequences. Due to a limited availability of scanner time, patient recruitment was extended over a 3-year period.

In conclusion, this study shows significant differences between two CMR perfusion sequences as applied according to guidelines, with advantage to the GRE-EPI-based hybrid sequence despite lower SNR and CNR than the SSFP perfusion sequence. The GRE-EPI sequence produces images that closely follow the variation in MPS signal, suggesting that objective evaluation of myocardial perfusion by CMR may be within reach.

## Acknowledgments

The technicians of the MRI and nuclear medicine units at Ryhov County Hospital, Jonkoping, are gratefully acknowledged for performing the patient studies. Siemens Healthcare gave access to the two perfusion sequences that at the time were work in progress, WIP. This study was supported by grants from the Medical Research Council of Southeast Sweden (Grant no 12437), Futurum, the County council of Jonkoping (Grants no 12440, 81851, 217261), Linkoping University, the County Council of Ostergotland (Grant no 281281) and the Swedish Heart-Lung Foundation (Grant no 20120449).

## Conflict of interest

The authors have no conflict of interest.

## References

Barkhausen J, Hunold P, Jochims M, *et al.* Imaging of myocardial perfusion with magnetic resonance. *J Magn Reson Imaging* (2004); **19**: 750–757.

Bratis K, Nagel E. Variability in quantitative cardiac magnetic resonance perfusion analysis. *J Thorac Dis* (2013); **5**: 357–359.

Carlsson M, Jogi J, Bloch KM, *et al.* Submaximal adenosine-induced coronary hyperaemia with 12 h caffeine abstinence: implications for clinical adenosine perfusion imaging tests. *Clin Physiol Funct Imaging* (2015); **35**: 49–56.

Cerqueira MD, Weissman NJ, Dilsizian V, *et al.* Standardized myocardial segmentation and nomenclature for tomographic imaging of the heart. A statement for healthcare professionals from the Cardiac Imaging Committee of the Council on Clinical Cardiology of the American Heart Association. *Int J Cardiovasc Imaging* (2002); **18**: 539–542.

Constantine G, Shan K, Flamm SD, *et al.* Role of MRI in clinical cardiology. *Lancet* (2004); **363**: 2162–2171.

Di Bella EV, Parker DL, Sinusas AJ. On the dark rim artifact in dynamic contrast-enhanced MRI myocardial perfusion studies. *Magn Reson Med* (2005); **54**: 1295–1299.

Finn JP, Nael K, Deshpande V, *et al.* Cardiac MR imaging: state of the technology. *Radiology* (2006); **241**: 338–354.

Fleischmann S, Koepfli P, Namdar M, *et al.* Gated (99 m)Tc-tetrofosmin SPECT for discriminating infarct from artifact in fixed myocardial perfusion defects. *J Nucl Med* (2004); **45**: 754–759.

Gebker R, Schwitter J, Fleck E, *et al.* How we perform myocardial perfusion with cardiovascular magnetic resonance. *J Cardiovasc Magn Reson* (2007); **9**: 539–547.

Gerber BL, Raman SV, Nayak K, *et al.* Myocardial first-pass perfusion cardiovascular magnetic resonance: history, theory, and current state of the art. *J Cardiovasc Magn Reson* (2008); **10**: 18. doi:10.1186/1532-429X-10-18

Gibbons RJ, Balady GJ, Bricker JT. ACC/AHA 2002 guideline update for exercise testing: Summary article: a report of the American College of Cardiology American Heart Association task force on practice guidelines (Committee to update the 1997 exercise testing guidelines). *J Am Coll Cardiol* (2006); **48**: 1731–1731.

Gould KL, Kirkeeide RL, Buchi M. Coronary flow reserve as a physiologic measure of stenosis severity. *J Am Coll Cardiol* (1990); **15**: 459–474.

Greenwood JP, Maredia N, Younger JF, *et al.* Cardiovascular magnetic resonance and single-photon emission computed tomography for diagnosis of coronary heart disease (CE-MARC): a prospective trial. *The Lancet* (2012); **379**: 453–460. doi: 10.1016/S0140-6736(11)61335-4.

Griswold MA, Jakob PM, Heidemann RM, *et al.* Generalized autocalibrating partially parallel acquisitions (GRAPPA). *Magn Reson Med* (2002); **47**: 1202–1210.

Gupta V, Kirisli HA, Hendriks EA, *et al.* Cardiac MR perfusion image processing techniques: a survey. *Med Image Anal* (2012); **16**: 767–785.

Gutberlet M, Noeske R, Schwinge K, *et al.* Comprehensive cardiac magnetic resonance imaging at 3.0 Tesla: feasibility and implications for clinical applications. *Invest Radiol* (2006); **41**: 154–167.

Hautvast GL, Chiribiri A, Lockie T, *et al.* Quantitative analysis of transmural gradients in myocardial perfusion magnetic resonance images. *Magn Reson Med* (2011); **66**: 1477–1487.

Hundley WG, Bluemke D, Bogaert JG, *et al.* Society for Cardiovascular Magnetic Resonance guidelines for reporting cardiovascular magnetic resonance examinations. *J Cardiovasc Magn Reson* (2009); **11**: 5.

Jerosch-Herold M. Quantification of myocardial perfusion by cardiovascular magnetic resonance. *J Cardiovasc Magn Reson* (2010); **12**: 57.

Jogiya R, Morton G, De Silva K, *et al.* Ischemic burden by Three-dimensional myocardial perfusion cardiovascular magnetic resonance: comparison with myocardial perfusion scintigraphy. *Circ Cardiovasc Imaging* (2014); **7**: 647–654.

Kellman P, Arai AE. Imaging sequences for first pass perfusion – a review. *J Cardiovasc Magn Reson* (2007); **9**: 525–537.

Kim HW, Farzaneh-Far A, Kim RJ. Cardiovascular magnetic resonance in patients with myocardial infarction: current and emerging applications. *J Am Coll Cardiol* (2009); **55**: 1–16.

Kramer CM. When two tests are better than one: adding late gadolinium enhancement to first-pass perfusion cardiovascular magnetic resonance. *J Am Coll Cardiol* (2006); **47**: 1639.

Kramer CM, Barkhausen J, Flamm SD, *et al.* Standardized cardiovascular magnetic resonance imaging (CMR) protocols, society for cardiovascular magnetic resonance: board of trustees task force on standardized protocols. *J Cardiovasc Magn Reson* (2008); **10**: 35.

Landis JR, Koch GG. The measurement of observer agreement for categorical data. *Biometrics* (1977); **33**: 159–174.

Marcassa C, Bax JJ, Bengel F, *et al.* Med EES-CWG, Nucl EA and Cardiovasc. Clinical value, cost-effectiveness, and safety of myo-

cardial perfusion scintigraphy: a position statement. *Eur Heart J* (2008); **29**: 557–563.

Merkle N, Wohrle J, Grebe O, *et al.* Assessment of myocardial perfusion for detection of coronary artery stenoses by steady-state, free-precession magnetic resonance first-pass imaging. *Heart* (2007); **93**: 1381–1385.

Mordini FE, Haddad T, Hsu LY, *et al.* Diagnostic accuracy of stress perfusion CMR in comparison with quantitative coronary angiography: fully quantitative, semiquantitative, and qualitative assessment. *JACC Cardiovasc Imaging* (2014); **7**: 14–22.

Nandalur KR, Dwamena BA, Choudhri AF, *et al.* Diagnostic performance of stress cardiac magnetic resonance imaging in the detection of coronary artery disease: a meta-analysis. *J Am Coll Cardiol* (2007); **50**: 1343–1353.

Sakuma H. Magnetic resonance imaging for ischemic heart disease. *J Magn Reson Imaging* (2007); **26**: 3–13.

Schwitter J, Wacker CM, van Rossum AC, *et al.* MR-IMPACT: comparison of perfusion-cardiac magnetic resonance with single-photon emission computed tomography for the detection of coronary artery disease in a multicentre, multivendor, randomized trial. *Eur Heart J* (2008); **29**: 480–489.

Schwitter J, Wacker CM, Wilke N, *et al.* Superior diagnostic performance of perfusion-cardiovascular magnetic resonance versus SPECT to detect coronary artery disease: the secondary endpoints of the multicenter multivendor MR-IMPACT II (Magnetic Resonance Imaging for Myocardial Perfusion Assessment in Coronary Artery Disease Trial). *J Cardiovasc Magn Reson* (2012); **14**: 61.

Taylor AJ, Cerqueira M, Hodgson JM, *et al.* ACCF/SCCT/ACR/AHA/ASE/ASNC/NASCI/SCAI/SCMR 2010 Appropriate Use Criteria for Cardiac Computed Tomography. A Report of the American College of Cardiology Foundation Appropriate Use Criteria Task Force, the Society of Cardiovascular Computed Tomography, the American College of Radiology, the American Heart Association, the American Society of Echocardiography, the American Society of Nuclear Cardiology, the North American Society for Cardiovascular Imaging, the Society for Cardiovascular Angiography and Interventions, and the Society for Cardiovascular Magnetic Resonance. *J Cardiovasc Comput Tomogr* (2010); **4**: 407 e401–407 e433.

Wang Y, Moin K, Akinboboye O, *et al.* Myocardial first pass perfusion: steady-state free precession versus spoiled gradient echo and segmented echo planar imaging. *Magn Reson Med* (2005); **54**: 1123–1129.

Zhang JJ, Raichlen JS, Kim SM, *et al.* Computer-assisted myocardial thickening analysis of gated MIBI SPECT images. *Invest Radiol* (1998); **33**: 257–262.